ELSEVIER

Journal of Alloys and Compounds 434–435 (2007) 628–632

Journal of ALLOYS AND COMPOUNDS

www.elsevier.com/locate/jallcom

Glass formation and magnetic characterization of $(Fe_{78}B_{14}Si_8)$–Nb–Y alloys

R. Piccin [a], P. Tiberto [b], M. Baricco [a,*]

[a] *Dipartimento di Chimica IFM and NIS, Università di Torino, Via P. Giuria, 9-10125 Torino, Italy*
[b] *IEN Galileo Ferraris, Strada delle Cacce 91, Torino I-10135, Italy*

Available online 17 October 2006

Abstract

In the present work, the glass formation of $Fe_{78}B_{14}Si_8$ alloy with small additions of Nb and Y has been investigated. Ribbons were prepared by planar-flow casting. Small ingots (up to 5 mm in diameter) were obtained by injection casting technique into a conical Cu mold. Thermal and structural properties were measured using differential scanning calorimetry (DSC) and X-ray diffraction (XRD), respectively. The microstructure has been observed by scanning electron microscopy (SEM). Quasi-static hysteresis loops have been measured using a vibrating sample magnetometer (VSM). Rapid solidification leads to a fully amorphous structure for all compositions. A partial amorphous structure has been obtained in samples prepared by copper mold casting, when adding Nb and Y. The role of Nb and Y addition on glass formation is discussed on the basis of melting behavior, analyzed by HT-DSC. Magnetic properties are correlated with the observed microstructures.

Keywords: Amorphization; Thermal analysis; Ferromagnetic materials

1. Introduction

Bulk metallic glasses (BMG) have been extensively studied due to their potential technological applications and their interesting physical properties [1]. In order to improve the glass forming ability (GFA), the minor alloying addition is a very effective method [2]. It was reported that Nb and Y improve the GFA of Fe-based alloys and their role has been related to thermodynamic, kinetic and structural effects [3,4].

Amorphous Fe–Si–B alloys are used as transformer core materials due to their good soft magnetic properties and the glass forming ability of these materials has been studied experimentally in the past [5]. More specifically, the most favorable Fe–Si–B glasses concerning their thermal stability have 5–10 at.% Si and 75–78 at.% Fe [6] and indeed, metallic glasses with the greatest technological significance are in this region [7]. However, the fully amorphous structure can be achieved below maximum thicknesses of 230 μm [5]. In order to improve the GFA of such alloys, the effect of small additions of Nb and Y has been investigated. The addition of a large atom such as Y helps to destabilize the competing crystalline phases due to its large negative heat of mixing with other small and intermediate atoms [8]. Moreover, Y was found to be able to scavenge oxygen from the undercooled liquid avoiding the heterogeneous nucleation and increasing furthermore the GFA. Nb addition enables the formation of stable amorphous phase through an increase in the stability of the supercooled liquid against crystallization due to its negative heats of mixing compared to Fe, Si and B [1,8].

This paper aims to investigate the role of addition of Nb and Y to a widely used magnetic amorphous alloy $Fe_{78}B_{14}Si_8$. The GFA has been analyzed comparing the results obtained by rapid solidification and by copper mold casting. It appears that the addition of both Nb and Y promotes bulk glass formation. The melting and solidification behavior of various alloys has been investigated by HT-DSC, showing a decrease of the melting temperature due to minor additions to the base alloy. From the SEM analysis of the microstructure of $(Fe_{78}Si_8B_{14})_{93}Nb_4Y_3$ master alloy, the presence of an immiscibility gap in the liquid state is inferred. The analysis of magnetic properties indicates a better behavior for the amorphous ribbon with respect to partially crystalline bulk metallic glass.

2. Experimental

$Fe_{78}Si_8B_{14}$, $(Fe_{78}Si_8B_{14})_{96}Nb_4$ and $(Fe_{78}Si_8B_{14})_{93}Nb_4Y_3$ master alloys have been prepared by arc melting 99.9% pure elements in a Ti-gettered argon

* Corresponding author. Tel.: +39 011 6707569; fax: +39 011 6707855.
E-mail address: marcello.baricco@unito.it (M. Baricco).

0925-8388/$ – see front matter © 2006 Elsevier B.V. All rights reserved.
doi:10.1016/j.jallcom.2006.08.272

atmosphere. The alloys have been melted several times in order to improve their homogenization. Ribbons with thicknesses between 30 and 60 μm have been prepared by planar-flow casting in Ar atmosphere. The master alloy was melted in a quartz crucible (with an open nozzle of 0.8 mm) using an induction coil and ejected thereafter in a cone-shaped Cu mold by applying an overpressure of about 0.15 bar. The bulk cast alloys have been prepared as cones with 5 mm base and 30 mm height.

The structure of the samples has been checked by X-ray diffraction (XRD) using Co Kα radiation. In the case of the cast cone-shaped ingots, the structural investigations have been performed on cone tips of 1 mm diameter. Alloys melting and solidification processes have been studied by using a Setaram HT-DSC at scanning rate of 0.033 K s^{-1}. The sample was introduced in an alumina pan and surrounded with alumina powder to prevent sticking to the crucible walls. The cell was evacuated and purged several times before measuring, under He flow. Calibration of the instrument has been performed by measuring the temperature and heat of fusion of samples of pure metals (Al, Ag, Au, Fe, Cu, Ni). The evolution of the crystallization process of the amorphous samples has been studied by Perkin-Elmer DSC7 using a heating rate of 0.33 K s^{-1} under Ar flow. Microstructure analysis has been carried out on samples previously etched with 2% Nital using a Leika Stereoscan 420 scanning electron microscope (SEM). Samples composition and homogeneity were verified by energy dispersive spectroscopy (EDS).

DC-magnetic measurements were carried out using a vibration sample magnetometer (VSM) in a maximum applied field of 1.5 T, at room temperature. The applied magnetic field was parallel to the casting direction of the samples. In the case of ribbons, the analyzed pieces with dimension of 3.0 mm × 3.0 mm × 0.050 mm were cut from a master ribbon. The measured cylindrical ingots had 1.0 mm diameter and 5.0 mm height.

3. Results and discussion

Fig. 1(a) shows the XRD patterns of the ternary $Fe_{78}Si_8B_{14}$ alloy (referred as base alloy hereafter). The presence of the ordered Fe_3Si (D03) and Fe_2B phases is observed in the master alloy. The formation of such phases was suppressed in rapidly solidified ribbons and the presence of a main halo indicates a fully glassy phase. In the ingot case, only bcc-Fe peaks are observed in the XRD pattern.

Fig. 1(b) shows the XRD patterns of the $(Fe_{78}Si_8B_{14})_{96}Nb_4$ alloy. bcc-Fe and a mixture of borides (Fe_2B, Fe_3B, $Fe_{23}B_6$) are observed in the master alloy. No Nb-containing phases were observed, suggesting the dissolution of this element in the equilibrium phases. The formation of borides was suppressed in the as-cast ingot and only diffraction peaks of bcc-Fe can be observed. Rapid solidification leads to a fully amorphous phase, as evidenced by the absence of diffraction peaks in the XRD pattern.

Fig. 1(c) shows the XRD patterns of the $(Fe_{78}Si_8B_{14})_{93}Nb_4Y_3$ alloy. Diffraction peaks corresponding to bcc-Fe, borides mixture (Fe_2B, Fe_3B, $Fe_{23}B_6$), $Fe_{17}Y_2$ and Fe_2Nb phases were identified in the master alloy pattern. Sharp crystalline peaks of bcc-Fe and borides, superimposed on a main amorphous halo, are observed for the as-cast 1 mm ingot, suggesting the presence of crystalline phases embedded in an amorphous matrix. The as-cast ribbon pattern presents only the main halo corresponding to a fully amorphous phase. A weak (2 0 0) diffraction peak of bcc-Fe is also observed in the pattern, indicating the presence of a small fraction of oriented crystals on the surface.

Fig. 2 shows the back-scattered SEM images of the microstructure of the $(Fe_{78}Si_8B_{14})_{93}Nb_4Y_3$ master alloy (a) and as-cast 1 mm ingot cross-section (b), respectively. The image of

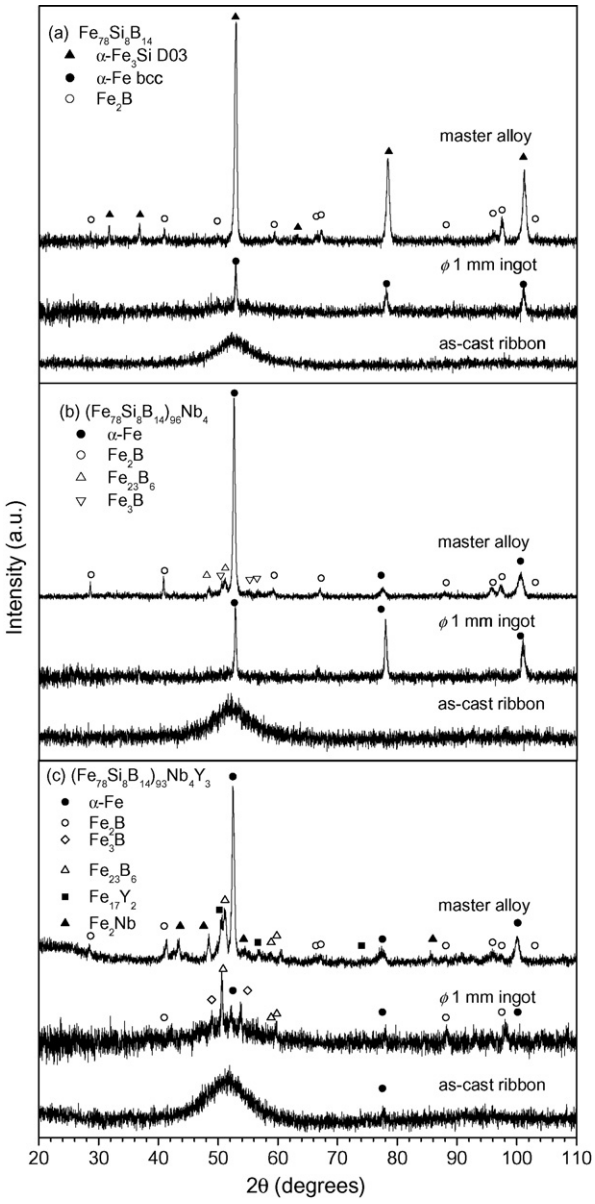

Fig. 1. XRD patterns of master alloy, as-cast 1 mm ingot and as-quenched ribbon: (a) $Fe_{78}Si_8B_{14}$, (b) $(Fe_{78}Si_8B_{14})_{96}Nb_4$ and (c) $(Fe_{78}Si_8B_{14})_{93}Nb_4Y_3$.

the master alloy indicates a heterogeneous microstructure spread over the whole sample and the presence of four equilibrium phases is clearly evidenced from the observed contrast. Equilibrium phases in the master alloy were identified from the chemical composition data measured in several areas of the sample. The brighter phase was identified as being Fe_2Nb (A), and concerning its drop-like shape, it is believed that this phase had solidified from a Nb-enriched liquid that has been separated from the parent liquid. Such liquid separation occurs due to presence of miscibility gap of the binary Nb–Y system that can be extended to more complex systems [9]. (B) and (C) areas in Fig. 2(a) were identified as bcc-Fe and boride phases, respectively, which were formed from a pseudo-eutectic reaction. A coarse $Fe_{17}Y_2$ microstructure (D) was also identified and it is expected to be formed from a solid-state reaction at low temperature. Fig. 2(b) shows a back-scattered image of a cross-section taken from the

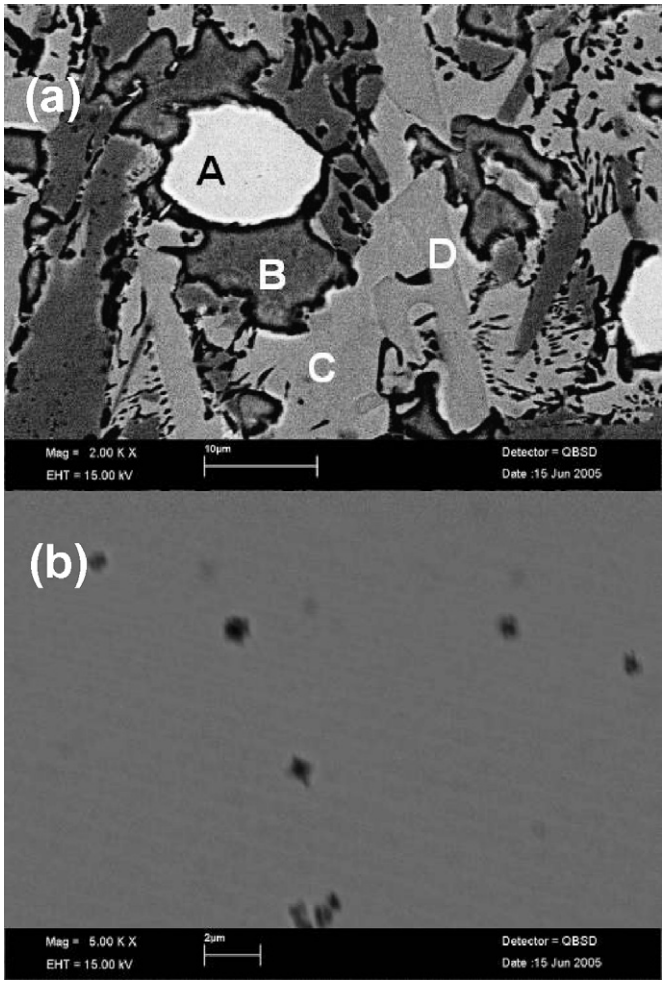

Fig. 2. Back-scattered SEM images of $(Fe_{78}Si_8B_{14})_{96}Nb_4Y_3$: (a) master alloy containing Fe_2Nb phase (A), bcc-Fe (B), boride phases (C) and $Fe_{17}Y_2$ phase (D); (b) as-cast 1 mm ingot cross-section.

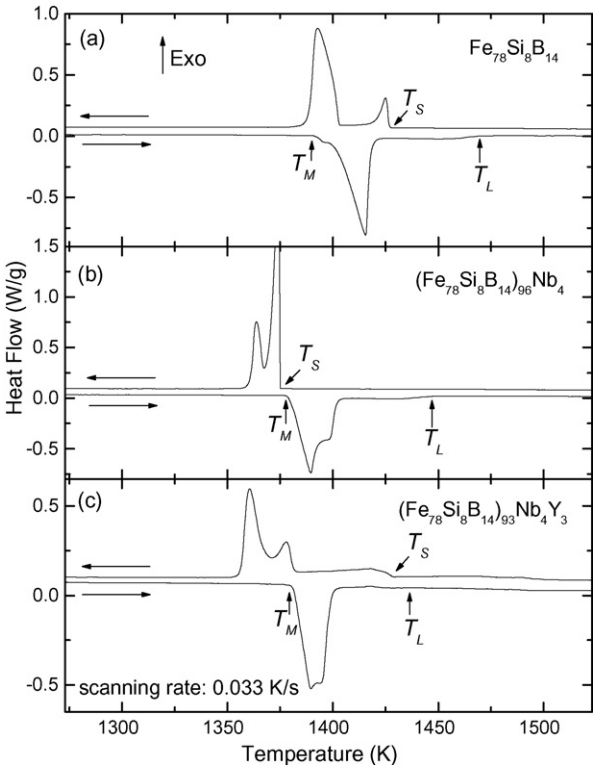

Fig. 3. High temperature DSC for (a) $Fe_{78}Si_8B_{14}$, (b) $(Fe_{78}Si_8B_{14})_{96}Nb_4$ and (c) $(Fe_{78}Si_8B_{14})_{93}Nb_4Y_3$ alloys. Arrows indicate T_M, T_R and T_L reported in Table 1.

tip of the as-cast $(Fe_{78}Si_8B_{14})_{96}Nb_4Y_3$ ingot. Only few spherical particles embedded in the amorphous matrix are observed. They cannot be easily identified by SEM, but according to XRD results they should correspond to a mixture of bcc-Fe and boride phases. SEM image of the cross-section of the ribbon (not shown here) did not show any significant contrast, confirming the formation of a fully amorphous phase by rapid solidification.

In order to understand the effect of Nb and Y addition on glass formation, the melting behavior of $Fe_{78}Si_8B_{14}$, $(Fe_{78}Si_8B_{14})_{96}Nb_4$ and $(Fe_{78}Si_8B_{14})_{93}Nb_4Y_3$ alloys has been investigated by HT-DSC. Melting and solidification curves are shown in Fig. 3 and the relevant thermal stability properties are collected in Table 1. The ternary base alloy (Fig. 3(a)) exhibits three endothermic peaks. According to the assessed Fe–Si–B phase diagram [10], the first peak (T_M) can be associated to the first melting reaction of the bcc-Fe/Fe_2B mixture. The main reaction corresponds to the melting of Fe_2B and it is followed by the liquidus point (T_L) at higher temperatures, where the bcc-Fe is fully transformed into the liquid. Solidification of the liquid alloy shows a slight undercooling, as evidenced by the huge exothermic signal due to primary solidification. Two solidification reactions, partially overlapped, follow without any significant undercooling. The DSC curve for the $(Fe_{78}Si_8B_{14})_{96}Nb_4$ alloy, shown in Fig. 3(b), displays that the first melting reaction, occurring at 1378 K, is the most intense and it is followed by an overlapped endothermic peak. Liquidus point was measured at 1448 K. Solidification of this alloy shows a strong liquid undercooling, as already observed for similar compositions [3]. For the $(Fe_{78}Si_8B_{14})_{93}Nb_4Y_3$ alloy the two melting reactions start at 1381 K and appear almost fully overlapped, as shown in Fig. 3(c). The liquidus point is barely visible on heating at 1436 K, but it is clearly observable, after a small undercooling, on the DSC trace of solidification. From the whole data of HT-DSC, it is clear that the addition of Nb reduces both T_M and T_L of the $Fe_{78}Si_8B_{14}$ alloy. The successive addition of Y to $(Fe_{78}Si_8B_{14})_{96}Nb_4$ does not influence significantly T_M and T_L values.

Fig. 4 shows DSC traces obtained for rapidly solidified ribbons and for the $(Fe_{78}Si_8B_{14})_{93}Nb_4Y_3$ ingot. The glass

Table 1
Thermal stability properties obtained from DSC traces

Alloy composition	T_M (K)	T_L (K)	T_S (K)	T_X (K)
$Fe_{78}Si_8B_{14}$	1392	1468	1427	830
$(Fe_{78}Si_8B_{14})_{96}Nb_4$	1378	1448	1375	844
$(Fe_{78}Si_8B_{14})_{93}Nb_4Y_3$	1381	1436	1428	948

T_M, melting temperature; T_L, liquidus; T_S, solidification temperature; T_X, crystallization temperature of amorphous ribbons.

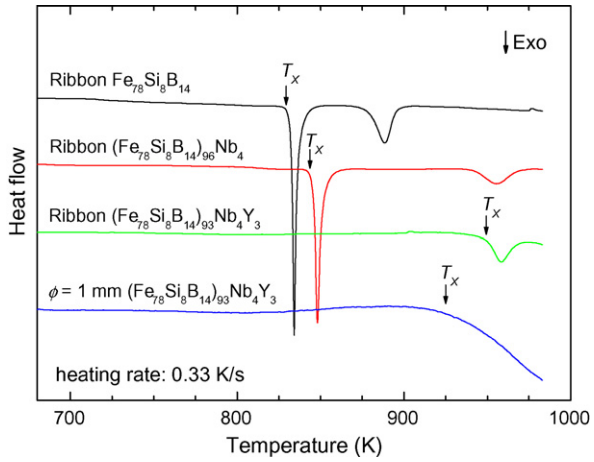

Fig. 4. DSC traces for as-quenched amorphous ribbons and $(Fe_{78}Si_8B_{14})_{93}Nb_4Y_3$ ingot.

transition temperature cannot be evidenced. The crystallization temperature (T_X) is marked by arrows on the DSC traces and the corresponding values are reported in Table 1. $Fe_{78}Si_8B_{14}$ and $(Fe_{78}Si_8B_{14})_{96}Nb_4$ alloys exhibit two resolved exothermal reactions. The first peak corresponds to the formation of α-Fe phase and the second one to the formation of Fe_2B phase [11]. Single exothermic peaks due to the crystallization of the glassy phase were found for $(Fe_{78}Si_8B_{14})_{93}Nb_4Y_3$ amorphous alloy in the temperature range accessible by the DSC7. The Nb addition to the base alloy increases T_X from 830 to 844 K and a further addition of Y increases T_X to 948 K for the ribbon and to 925 K for the ingot.

The magnetization curves of the as-quenched ribbons and as-cast 1 mm ingot are shown in Fig. 5 for: (a) $Fe_{78}Si_8B_{14}$, (b) $(Fe_{78}Si_8B_{14})_{96}Nb_4$ and (c) $(Fe_{78}Si_8B_{14})_{93}Nb_4Y_3$ alloys. The measurements were performed with a maximum applied field of 15 kOe. The saturation magnetization (M_S), coercive field (H_C) and magnetic susceptibility (χ_M) of ribbons and as-cast ingots are presented in Table 2. The addition of Nb and Y decreases M_S values of the fully amorphous ribbons. Such a decrease

Table 2
Magnetic properties of $Fe_{78}Si_8B_{14}$, $(Fe_{78}Si_8B_{14})_{96}Nb_4$ and $(Fe_{78}Si_8B_{14})_{93}Nb_4Y_3$ alloys

Alloy composition	Ribbon	CM ingot (1 mm)
M_S (emu g^{-1})		
$Fe_{78}Si_8B_{14}$	159	165
$(Fe_{78}Si_8B_{14})_{96}Nb_4$	147	180
$(Fe_{78}Si_8B_{14})_{93}Nb_4Y_3$	116	137
H_C (Oe)		
$Fe_{78}Si_8B_{14}$	1.1	21
$(Fe_{78}Si_8B_{14})_{96}Nb_4$	0.7	79
$(Fe_{78}Si_8B_{14})_{93}Nb_4Y_3$	0.7	20
χ_M (emu g^{-1} Oe^{-1})		
$Fe_{78}Si_8B_{14}$	0.98	0.13
$(Fe_{78}Si_8B_{14})_{96}Nb_4$	2.00	0.18
$(Fe_{78}Si_8B_{14})_{93}Nb_4Y_3$	1.20	0.21

M_S, saturation magnetization; H_C, coercive field; χ_M, magnetic susceptibility.

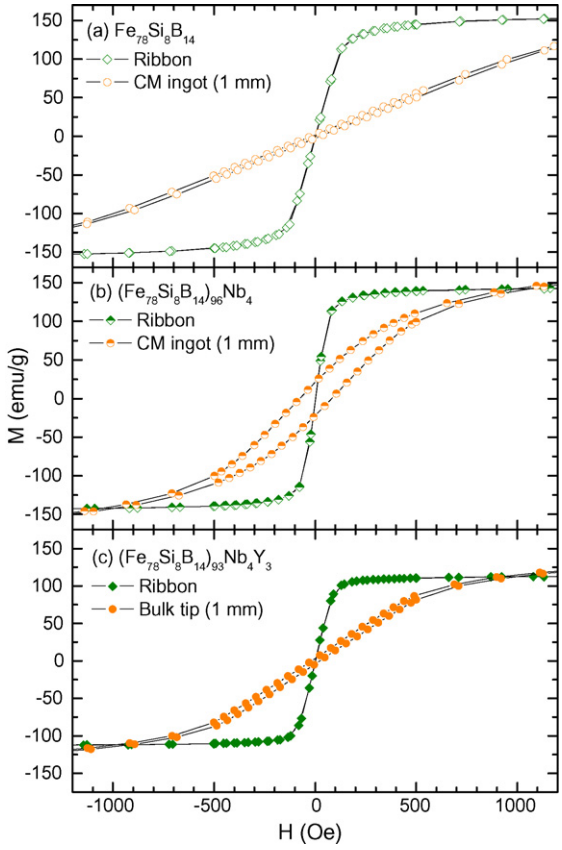

Fig. 5. Magnetization curves of as-cast ingot and as-quenched ribbon: (a) $Fe_{78}Si_8B_{14}$, (b) $(Fe_{78}Si_8B_{14})_{96}Nb_4$ and (c) $(Fe_{78}Si_8B_{14})_{93}Nb_4Y_3$.

can be explained by the presence of non-magnetic atoms inside the glassy phase, which changes the magnetic response of the matrix. In the case of the as-cast ingot, M_S changes are explained according to the concentration of bcc-Fe inside the ingot. For both ribbons and ingots, only the double addition of Nb and Y causes important decrease of M_S. Single Nb addition does not change significantly M_S values. Typical magnetically soft H_C values were obtained for ribbons of all compositions and slight decreases were observed when Nb and Y are added. Comparing the coercive fields of each ribbon with the respective ingot, a significant raise is noted for the last one. Such a raise is due to the presence of crystalline α-Fe and borides mixture, in agreement with the measured XRD patterns. In the particular case of Nb addition, the raise is more pronounced and it is believed that Nb atoms exert large stress in the crystalline phase [12]. Comparing the magnetic susceptibility of the ribbon and the as-cast ingot, in all cases the ribbons exhibit larger values, which is explained by the higher cooling rates assured in the ribbons preparation technique.

4. Conclusions

The effect of small additions of Nb and Y on glass formation of the ternary $Fe_{78}Si_8B_{14}$ alloy has been examined. Fully amorphous ribbons were obtained by rapid solidification. Partially glassy 1 mm ingots were obtained by adding 4 at.% Nb

and 3 at.% Y, as confirmed by XRD and DSC measurements. The high temperature DSC analysis showed that the addition of Nb and Y lowers the melting temperature and increases the undercooled liquid region of the alloys.

The magnetic measurements indicate a soft magnetic behavior for the as-cast ribbons. The saturation magnetization of the as-cast ribbons decreases with the addition of Nb and Y due to the presence of non-magnetic atoms inside the amorphous phase. The presence of boride crystals embedded in the amorphous matrix in 1 mm ingot of $(Fe_{78}Si_8B_{14})_{93}Nb_4Y_3$ appears strongly detrimental for the soft magnetic properties.

Acknowledgments

Work performed for COFIN/MIUR 2005097983_002 and for MRTN-CT-2003-504692. RP is supported by the Programme Alβan, the European Union Programme of High Level Scholarships for Latin America, scholarship no. E04D036521BR.

References

[1] N. Nishiyama, K. Amiya, A. Inoue, Mater. Trans. 45 (2004) 1245.
[2] Z.P. Lu, C.T. Liu, J. Mater. Sci. 39 (2004) 3965.
[3] A. Inoue, B. Shen, Mater. Trans. 43 (2002) 766.
[4] D.S. Song, J.-H. Kim, E. Fleury, W.T. Kim, D.H. Kim, J. Alloys Compd. 389 (2005) 159.
[5] M. Mitera, M. Naka, T. Masumoto, N. Kazama, H. Watanabe, Phys. Status Solidi (a) 49 (1978) 163.
[6] K. Chrissafis, M.I. Maragakis, K.G. Efthimiadis, E.K. Polychroniadis, J. Alloys Compd. 386 (2005) 165.
[7] I. Matko, E. Illekova, P. Svec, P. Duhaj, Mater. Sci. Eng. A 225 (1997) 145.
[8] F.R. de Boer, R. Boom, W.C.M. Matterns, A.R. Miedema, A.K. Niessen, Cohesion in Metals, North-Holland, Elsevier Science Publishers B.V, Amsterdam, 1988.
[9] N. Mattern, U. Kuhn, A. Gebet, T. Gemming, M. Zinkevich, H. Wendrock, L. Schultz, Scripta Mater. 53 (2005) 271–274.
[10] T. Tokunaga, H. Ohtani, M. Hasebe, Calphad 28 (2004) 354.
[11] D.S. dos Santos, D.R. dos Santos, J. Non-Cryst. Solids 304 (2002) 56.
[12] R.S. Turtelli, M. Schonhart, H. Sassik, R. Grossinger, C. Kolbeck, Vo Hong Duongm, E. Ferrara, J. Magn. Magn. Mater. 226–230 (2001) 1498–1500.